

# **Field Demonstration of Ion Trap for Aerosol Characterization: Interim Report**

**Project Number: 30337**

Stephan E. Barlow and Michael L. Alexander  
W.R. Wiley Environmental Molecular Sciences Laboratory  
Pacific Northwest National Laboratory  
Richland, WA 99352

## **Summary:**

We report here our progress to date on the development and construction of a field deployable aerosol mass spectrometer. This report describes work on several fronts including theoretical developments, trap design and construction, laboratory studies with existing equipment and some related, but not necessarily project supported activities that directly impinge on this project.

Much of the body of this report is rather technical, to assist the reader who may be unfamiliar with RF ion trap mass spectrometers, we include as a separate document a brief primer on the theoretical underpinning of this technique. The primer is a much older document prepared prior to the beginning of this project.

## I. Introduction

In the following pages, we detail work conducted by us on ion trap development. The goal of the project is to produce a useful and fieldable Ion trap mass spectrometer for determining the composition of atmospheric aerosols. The instrument will function by introducing aerosol-containing air through a differentially pumped interface. Aerosols are first detected and sized by a two laser scattering targeting system. Analysis is to be accomplished by triggered laser desorption/ionization of the targeted aerosol, followed by mass analysis of the resulting ion cloud using the new asymmetric ion trap developed at PNNL. Analysis of each particle will include both cation and anion spectra.

The asymmetric ion trap we have developed at PNNL was originally intended for aerosol or other solids analysis. The “asymmetry” itself was introduced to reduce shot-to-shot “peak bounce” inherent in earlier ion trap designs. This needs a little explanation. One of the major limits of RF ion trap mass spectrometers is the fact that from one measurement to the next, using nominally identical ionization and analysis conditions and the same analyte, considerable variation in mass peak heights is observed. (This is a bit of an “insiders’” secret and little or no discussion of this problem can be found in the open literature.) Of course, such a state of affairs makes the RF trap unsuitable for many environmental applications, where the analyte can change with each cycle. Further, this problem obviates a major attractive feature of the RF trap, namely the ability to do simultaneous cation and anion mass spectroscopy.

An obvious source of “peak bounce” is the plane of symmetry that standard traps possess. Ions can just as easily exit the trap opposite to the detector as toward it. Our asymmetric trap virtually eliminates this possibility. We now come to the first rule of instrument improvement: *“Having eliminated one major source of noise (or other difficulty) I can now see all of the other noises much more clearly.”* “Peak bounce” comes not only from the exit direction, but also from finer details of the trajectory. For instance, ions can be ejected with a very wide spread of kinetic energies. Low energy ions will tend to find their way to the exit electrode and be lost, while high energy ions cannot be bent into the detector. The energy spread is a function of minute details of the ions’ trajectories and can vary wildly from one measurement to the next. Thus much of this work is focussed on understanding the energy spread.

## II. Theory and Modeling Activities

Although this project is primarily a design and construction activity, our philosophy from the beginning has been to allow basic theoretical principles guide the design wherever possible. This approach has proven itself time and again, especially where it results in a deeper understanding of what aspects of design and operation are important and what aspects require less importance. These principles for instance led to the asymmetric ion trap design in the first place. Further, the literature of RF ion trap mass spectrometry is replete with both theory and experiment, but only very seldom do these activities seem to

have converged in instrument design and operational specifications. In this project, time is short and the needs rather substantial—no one has ever built an instrument quite like this one. Thus to speed the design work and to give guidance to the later laboratory testing protocol we have undertaken a very modest theoretical and modeling effort.

Despite its small scope we have already had major results. These results include:

- A. Understanding the tolerancing of the trap structure—very important
- B. Importance of truncation and electrode flanging—minor importance
- C. Reduction of ejected ion energy spread—important to minimize “peak bounce”
- D. Effects of holes through end caps—necessary evils
- E. Effects of “non-ideal” spacing used in commercial instrumentation—we don’t seem to need it.
- F. Effect of access slots for particle introduction and laser desorption—these largely compensate the holes
- G. Effects of the truncated, asymmetric trap
- H. Effects of buffer gas in ion relaxation

## II. a. Calculation of Trapping Fields

Beaty<sup>1</sup>, Gabrielse<sup>2</sup> and Franzen<sup>2</sup> have done detailed calculations on the effects of electrode truncation, the first two authors sought to produce trapping fields that were as close to ideal as possible, while Franzen made the realization that the anharmonicities could be intentionally added and exploited for mass spectroscopy. In all cases these authors used very sophisticated electrostatic codes which they spend considerable time and effort developing. Unfortunately for us, none of them seemed to have paid much attention to the effects of the small holes in the end cap electrodes that are necessary for ion ejection from a Paul trap. (In all fairness, this issue was irrelevant to both Beaty and Gabrielse.) Further complicating the issue of electric fields here is the effect of the large slots in the ring electrode.

Rather than developing our own electrostatic code we employed SIMION<sup>4</sup> and wrote only a small code to extract the electrostatic potentials. This approach has certain fundamental limitations, such as fixed grid sizes that limit the precision to which surfaces may be specified. (This had the ironic advantage of giving us an estimate of tolerancing requirements: Surfaces must be located with an absolute precision that exceeds 0.5 part per thousand, and surface roughness must be reduced as much as possible.) Figure 1 illustrates the specific geometries that we report on in Table 1. Once the potentials were calculated

We constructed a cylindrical Gaussian surface inside the trapping volume, see Fig. 2. The cylinder dimensions were chosen to be a few grid points away from the nearest wall to reduce numerical “noise” due to the grid’s coarseness. The potentials  $\Phi(R_0, z)$  and  $\Phi(r, Z_0)$ , on the faces of the cylinder were then used to calculate the Potential interior of the cylinder  $\Phi(r, z)$ .

$$\Phi(r, z) = \sum_{n=0}^{\infty} a_n I_0\left(\frac{[2n+1]pr}{2Zo}\right) \cos\left(\frac{[2n+1]pz}{2Zo}\right) + \sum_{n=0}^{\infty} b_n J_0\left(\frac{j_n r}{Ro}\right) \cosh\left(\frac{j_n z}{Ro}\right)$$

Where  $a_n$  and  $b_n$  are determined from the calculated boundary values. (This equation becomes somewhat more complex when the potentials for the asymmetric trap are evaluated. Having found  $\Phi(r, z)$  in this form, the Bessel and trig functions can then be expanded in Taylor series and regroup in the form of a multipole expansion of Laplace's equation:

$$\begin{aligned} \Phi(r, z) = & \Phi_0 + \frac{c_1 V}{Ro} z + \frac{c_2 V}{Ro^2} (r^2 - 2z^2) + \frac{c_3 V}{Ro^3} (r^2 z - \frac{2}{3} z^3) + \\ & \frac{c_4 V}{Ro^4} (r^4 - 8r^2 z^2 + \frac{8}{3} z^4) + \frac{c^5 V}{Ro^5} (r^4 z - \frac{8}{3} r^2 z^3 + \frac{8}{15} z^5) + \\ & + \frac{c^6 V}{Ro^6} (r^6 - 18r^4 z^2 + 24r^2 z^4 - \frac{16}{5} z^6) \end{aligned}$$

Where the  $c$ 's are dimensionless constants. This procedure although apparently complex is actually rather rapid as is the convergence for the low-order  $c$ 's. More importantly, this procedure produces a unique solution, which from basic mathematical theory must be correct. Note that we have assume cylindrical, but not axial symmetry. For axially symmetric traps, all of the odd terms in  $z$  are zero and the problems simplifies. As Franzen has pointed out, these odd terms do not contribute significantly to particle dynamics<sup>5</sup> and so need not enter directly into our analysis. (In passing we note that their presences in the actual potentials determined from the calculation is a measure of the coarseness of the grid used in the initial determination of  $\Phi(r, z)$  .

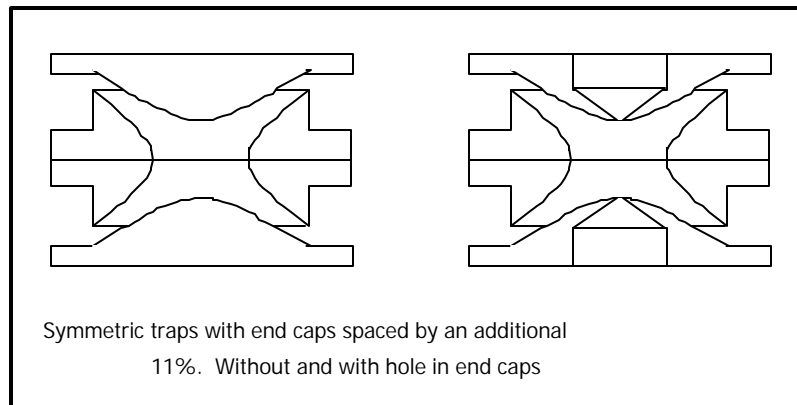
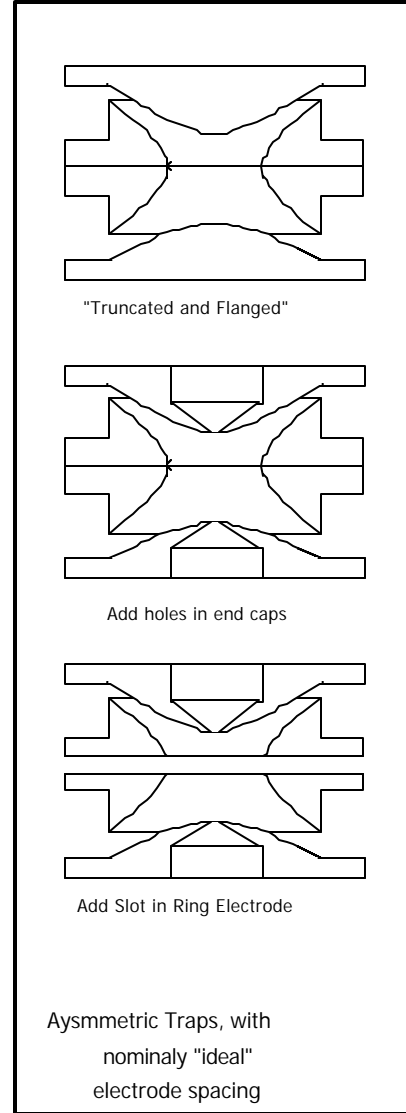
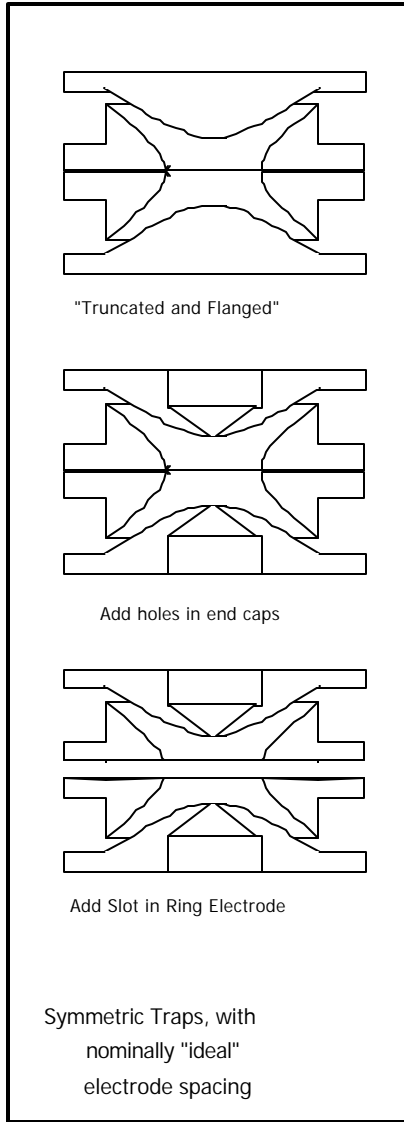


**Figure 1.** Trap Geometries Treated in calculations of trapping field see text ant Table 1 for discussion.

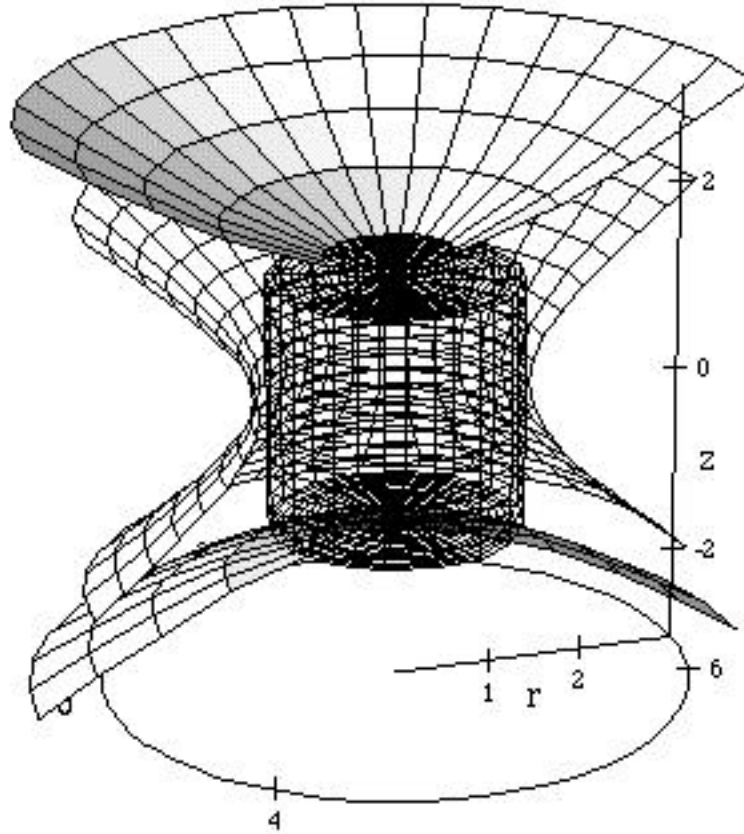


**Figure 2.** Illustration of Gaussian surface (wire framed cylinder) constructed inside of hyperbolic electrode.

Data for the low order even terms of the traps illustrated in Figure 1 is presented in Table 1. It is the low order anharmonic terms that will tend to dominate the deviations of trap performance from the expected ideal. The origins of the commercial trap with additional spacing has been discussed at length by Syka<sup>6</sup> and investigated at greater length by Cooks and coworkers.<sup>7</sup> Several rather surprising results emerge from these calculations. First, the “commercial spacing” trick does not minimize the anharmonicities, but it does cause the value of  $C_4$  to change signs. Secondly, the addition of the ring slits, whether to the standard symmetric trap or the asymmetric trap, produces field anharmonicities that are nearly identical with the stretched geometry in both  $C_4$  and  $C_6$ . This does not explain why the fields are found as a practical matter to be more desirable than ones closer to the ideal or purely harmonic ones, but it does indicate that we should expect similar performance. (We are currently working on proposals to extend this investigation.)

<b>Table 1: Trap</b>	$\Phi_0$	$C_2$	$C_4$	$C_6$
Canonical Spacing	0.500715	0.49991	4.8038 E-05 • 0	-3.5426 E-04 • 0
Canonical Spacing w/endcap holes	0.500950	0.49916	1.7665 E-03	-4.1801 E-03
Canonical Spacing w/endcap holes, and ring slit	0.483804	0.47801	-9.2535 E-3	-1.554 E-2
“Commercial” Spacing w/endcap holes	0.540780	0.42976	-1.5125E-2	-9.5926 E-3
Asymmetric Trap	0.500688	0.50001	-8.8286 E-5 • 0	-2.6616 E-4 • 0
Asymmetric Trap w/endcap holes				
Asymmetric Trap w/endcap holes and slits	0.481841	0.48068	-1.1002 E-2	-1.3332 E-2

## II. b. Ion Production, Relaxation and Mass Selective Ejection

High quality mass spectra from an ion trap require a careful balancing of several competing needs. Presumably, the nascent ion population, i.e., immediately after the ionization event is the most meaningful and accurate representation of the analyte's composition. With time, ions can react with background neutral gases and anion/cation recombination will occur. On the other hand, for the ion trap to work well as a mass spectrometer, the ion population must be relaxed to a near thermal distribution. Further, just as in any form of spectroscopy, the more rapid the spectrum is scanned, the lower the resolution. Finally, the need for sample throughput generally requires rapid response. Fortunately, for our purposes, there exists a fairly convenient time window, on the order of 50-200 ms where these competing requirements can be met. Typically a helium buffer gas at a few times  $(10)^{-5}$  will relax most ion populations in about 10 ms. If the ion density is not too high, and the buffer is clean, very little ion-molecule reaction occurs and recombination is only modest. Thus experience indicates that reasonable spectra can be obtained. The quality of the mass spectra can also be improved through carefully controlled ionization techniques. In our case, this generally means using very modest laser powers for desorption and ionization and carefully controlling “where” in the trap the ionization event takes place. (Battelle Proprietary result). It is also critical to monitor the laser power and use high quality beams.

Once ions have been produced and stored a mass spectra is generated by sequentially ejecting ions through the end cap hole to the detector. The asymmetric ion trap design, assures that all of the ejected ions leave through the detection-side end cap. However, the

“mode” of ion ejection can strongly affect the signal quality. Table 2 is a list of ejection options together with some of the pro’s and con’s of each technique.

<b>Table 2.</b> Mass Selective Ion Ejection options	Pro’s	Con’s
Instability Ejection	Well developed, “standard”	Very large ion energy spread. Poor peak shape
Secular assisted instability ejection	Well developed, improved peaks	Large ion energy spread
Fixed frequency resonance secular ejection <sup>†</sup>	Well developed, when secular resonance frequency is properly chosen	Large numbers of low energy ions, strongly affected by anharmonicities
Swept frequency secular ejection	Very small RF requirements	Poorly developed, loss of resolution at high masses
Swept or fixed frequency micromotion excitation	None known	Not investigated

<sup>†</sup> Probable choice here

Several factors combine to make these considerations of greater than usual importance. First, we wish to implement simultaneous anion/cation detection. This means that the detectors must be located off-axis from the trap and therefor, ion must be steered to their respective targets. Ions with too little energy will simply be lost to the exit trap electrode, while those with too much energy cannot be steered. Second, ions of identical mass should leave the trap more or less together, some ejection schemes are strongly dependent on the relative phase of the ion motion with respect to the trapping RF field and very large dispersions of ejection times (and energies) can result. These effects are generally well known in the RF trap community and are readily reproduced in simulations. The simulations and experiments using fixed frequency resonance secular ejection where the secular resonance frequency is chosen to be 1/3 of the RF trapping frequency, seems to give excellent results. This choice of parameters has been discussed by Franzen, et al.<sup>8</sup> Because a simple harmonic relation exists between the RF trapping frequency and the secular resonance drive, a definite phase relationship between the two is guaranteed. In the presence of a damping gas, the secular drive will then tend to bring resonance ions into a definite phase relationship as well. By carefully choosing and controlling these relationships, peak shapes and mass resolution can be optimized. It is during the last few cycles of the ions’ orbits that the anharmonic terms become important. This is due to the fact that ejection is accomplished by sweeping a field parameter, usually the RF trapping amplitude.

At this point we can appreciate better the importance of anharmonicities that were discussed above. If the sign of the anharmonicity is unfavorable, the ions will quickly move out of resonance with increasing orbital amplitude and produce poorly shaped peaks. On the other hand, if the magnitude of the anharmonicities is too large, the trap will exhibit amplitude dependent instabilities and ions will tend to be ejected with large energy spreads.



### III. Instrument Design and Construction

In parallel to the theoretical considerations outlined above, the new instrument has been designed and construction is nearing completion. Figures 3 and 4 show assembly drawing of the trap structure and the detector mountings. The whole arrangement and design is considerably simpler than most commercial instruments, with one exception. We have incorporated three axis adjustable mounts on the two detectors. This will allow us to find optimal settings for their locations. In future designs the detectors will probably be fixed thereby much reducing cost and complexity. We have also incorporated a compact re-entrant einzel lens in the exit electrode. We anticipate that it will be useful in quickly extracting ejected ions and assist in directing them to the appropriate detector.

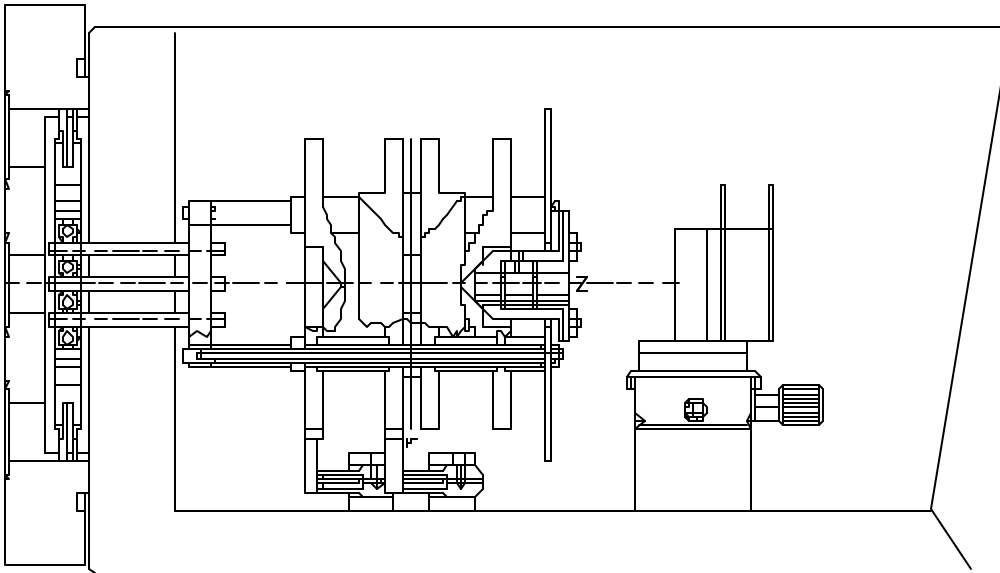


**Figure 3.** Elevation of Trap Structure and Detector mount.

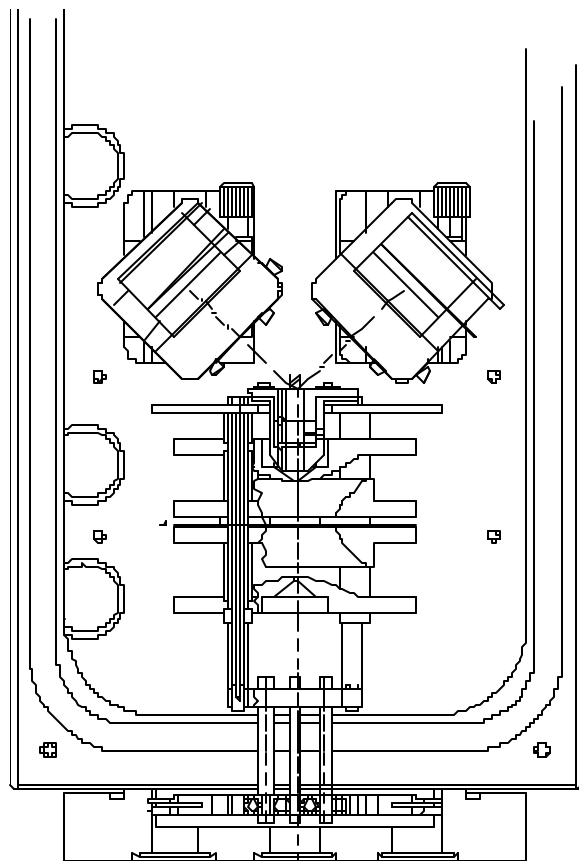


**Figure 4.** Top View of Asymmetric Ion Trap showing flange and detector mounts.

### III. Experimental Activities

#### Laser desorption ion trap mass spectroscopy

We have used the existing trap and laboratory equipment to conduct preliminary tests of laser desorption and to compare chemical analysis in the ion trap with existing methods. The first system chosen was a sample of the mineral Augite. This particular sample has been well characterized by standard methods including ICP-MS. A mass spectrum taken at laser desorption wavelength of 266 nm is shown in Figure 5 below.

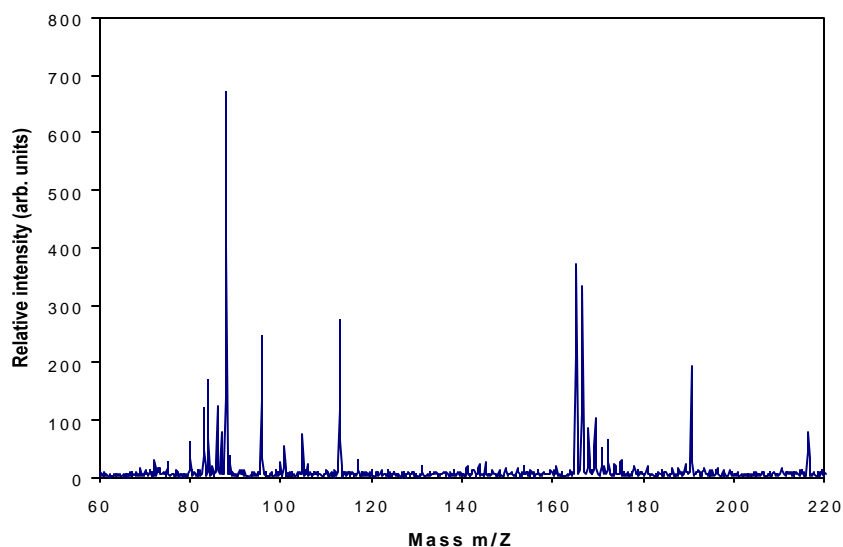


**Figure 5.** Mass spectrum from laser desorption of Augite inside ion trap

This spectrum is from a single laser shot, demonstrating the excellent signal to noise and sensitivity. The relative concentrations of various elements (including Rb, Sr, Nd, Ho, and Pb) range from less than 1 ppm to 100 ppm and are in excellent agreement with ICP-MS data. This sensitivity is more than adequate to obtain the chemical information required for particle characterization. Further verification of the quantitative ability of the laser desorption ion trap system is shown in figures 6 and 7.

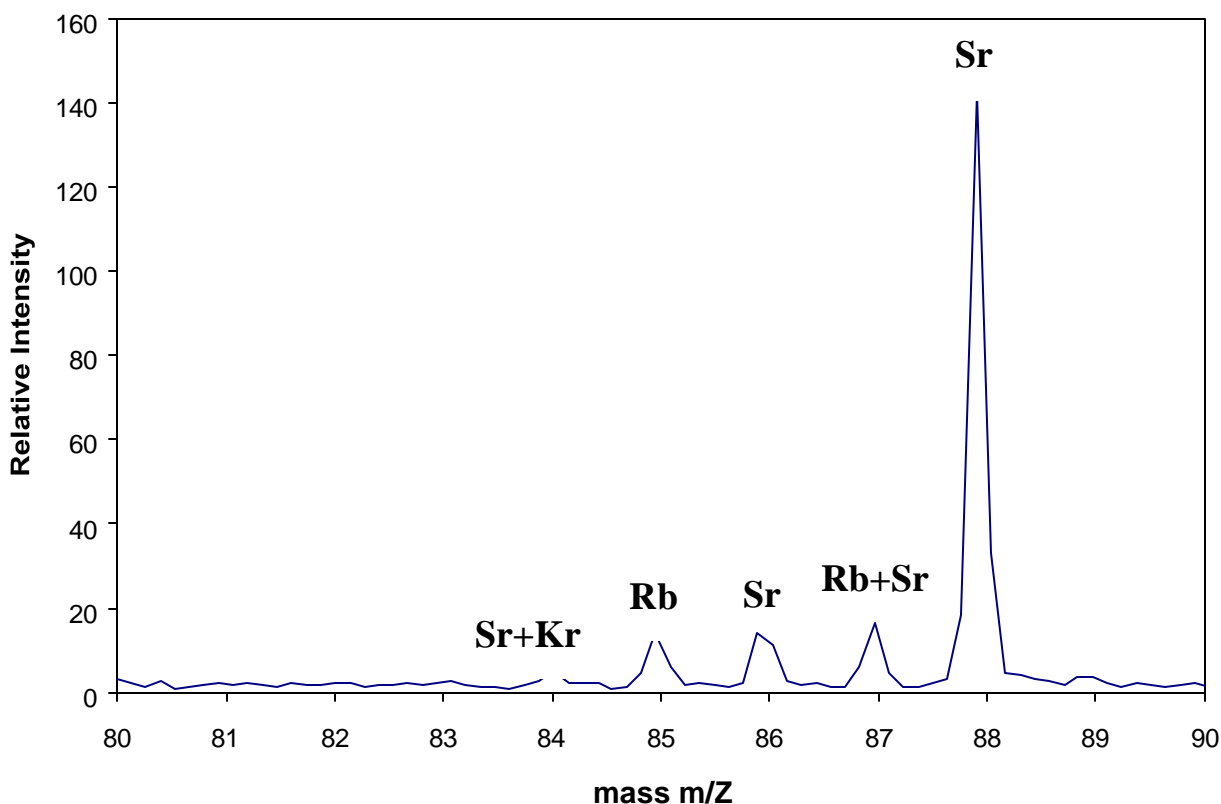


**Figure 6.** Mass spectrum from laser desorption of Augite at 532 nm with isotope assignments in region from mass 80 to 90

Figure 6 shows the  $m/Z$  region from 80 to 90 resulting from laser desorption at 532 nm. This wavelength was chosen because 266 nm is resonant with transitions in Sr and skews the elemental ratio. The relative peak heights are in excellent agreement with calculated values based on known natural isotope ratios as shown in figure 7. These results are much better than those obtained using ICP-MS scanning quadrupole methods due to the single shot nature of the data acquisition. The discrepancy at mass 84 is due to interference from another element, probably Kr. This was not included in the calculation of relative peak heights. The excellent agreement is largely due to the ability to acquire data on a single-shot basis, allowing consistent measurement of elemental and isotopic ratios. This ability will be crucial for performing single particle analysis.

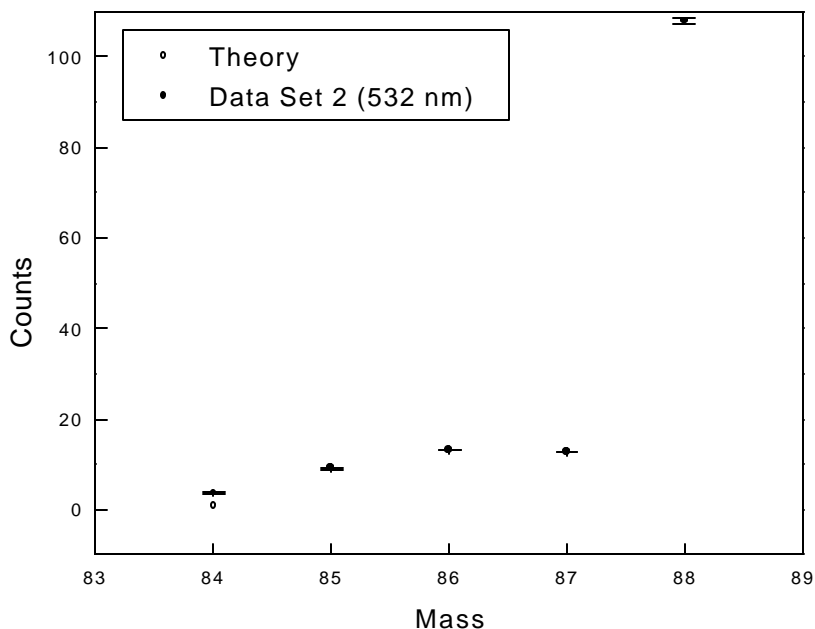


**Figure 7** Peak heights calculated from known concentrations and isotope ratios for Sr and Rb compared to observed values

#### Optical detection and sizing of particles

A crucial component in the PNNL particle measurement system is the measurement of particle size correlated with the mass spectrum, or compositional analysis. Previous efforts to do this have relied on a two-laser system to measure each particle's velocity. This measurement gives the aerodynamic size of the particle as well as providing a timing signal for synchronizing the desorption laser.

We have done initial tests on a system that uses fast optical detection to simultaneously measure the velocity, yielding the aerodynamic particle size, as well as the optical light scattering cross section, using a single laser. This provides information on the size, shape and density of the particle, more than is currently obtained for two-laser velocimetry measurements. The details of this system are proprietary, but can be discussed after proper documentation is in place.

#### **IV. Other Related Activities**

This project has garnered considerable outside interest. Early in June 99, one of us (S.E. Barlow) attended the Tropospheric Aerosol Program (TAP) Workshop, the purpose of this workshop was to plan a new program within the DoE Office of Biological and Environmental Research (OBER) and was held at Brookhaven National Laboratory. Discussion of this project generated considerable interest and the TAP program plan explicitly recognizes the need for real-time chemical characterization of aerosols. (Section 5.2).

Both M.L. Alexander and S.E. Barlow attended the 47<sup>th</sup> American Society for Mass Spectrometry meeting in Dallas, TX in mid-June 99. There we presented a poster that summarized our work to that date. Once again, the project elicited considerable interest on the part of academic, government and commercial researchers.

As a part the PNNL technology transfer and local economic development programs, the asymmetric trap technology is likely to be commercially licensed in the near future. Given the interest in aerosol analysis that exists, we anticipate that some variant of the aerosol mass spectrometer will become commercially available within a few years.

## **References**

1. E.C. Beaty, J. Appl. Phys., **61** (1987) 2118
2. G. Gabrielse, , Phys Rev. A, **27** (1983) 2277
3. Y. Wang, J. Franzen, K.-P. Wanczek, Int. J. Mass Spectrom. Ion Proc., **112** (1993) 125
4. D.Dahl, SIMION,v6.0,
5. L. Landau and Lifshitz, "Mechanics," Pergammon Press, 19\_\_, page\_\_.
6. J.E.P. Syka, "Practical Aspects of Ion Trap Mass Spectrometry, Vol I," R.E. March and J.F.J. Todd, eds., CRC Press, Boca Raton, 1995, Ch 4, pg 169.
7. L.A. Gill, J.W. Amy, W.E. Vaughn and R.G. Cooks, Int. J. Mass Spect. Ion Proc., **188** (1999) 87.
8. J. Franzen, R.H. Gabling, M Schubert and Y. Wang, "Practical Aspects of Ion Trap Mass Spectrometry, Vol I," R.E. March and J.F.J. Todd, eds., CRC Press, Boca Raton, 1995, Ch 3, pg 49.

## **Other Participants:**

Calculations: Ms. Aimee Taylor, summer intern, Dr. Viktor Pervukin, visiting scientist

Design and Drafting: Mr. Mathew Covert, draftsman

Electronic Design: Mr. Jim Follansbee, electrical engineer

Software Design: Dr. John Price, chief of EMSL Instrument Development Laboratory

Laboratory Measurements: